World Journal of Advanced Engineering Technology and Sciences
eISSN: 2582-8266
Cross Ref DOI: 10.30574/wjaets
Journal homepage: https://wjaets.com/

(RESEARCH ARTICLE)

Effect of particles size variation of graphite on mechanical properties of piston materials

Sunday Olufemi Adetola, Ayodele James Oyejide *, Uthman Abdufatai Olatunde, Lala Ayomide Isaac and Ayinde Kehinde James

Department of Mechanical Engineering, Ladoke Akintola University of Technology, Ogbomoso, Oyo State, Nigeria.

World Journal of Advanced Engineering Technology and Sciences, 2024, 12(02), 424–434

Publication history: Received on 10 April 2024; revised on 23 July 2024; accepted on 25 July 2024

Article DOI: https://doi.org/10.30574/wjaets.2024.12.2.0299

Abstract

This work investigates the influence of varying graphite particle sizes on the mechanical properties of pistons, crucial components of internal combustion engines. Graphite sourced from used batteries were ball milled for durations of 3, 6, and 9 hours to achieve size reduction. These milled graphite particles are then dispersed into molten pistons to create composites. Additionally, a control sample comprising an aluminum (AI) alloy without graphite is included for comparison. Particle size analysis reveals graphite sizes of 125 µm, 90 µm, and <90 µm for milling durations of 3, 6, and 9 hours, respectively. The chemical composition of the ingot used as the base material for the pistons comprises 85% Al, 11.37% Si, and trace elements. The composite pistons undergo testing for hardness and tensile strength, with results indicating significant enhancement in mechanical properties with decreasing graphite particle size. Specifically, compared to the control sample, the composite with graphite particles <90 µm exhibits a notable 53% increase in tensile strength (140.44 MPa) and a 2.5% increase in hardness (48.67 HRB). These findings emphasize the potential for optimizing piston performance by controlling graphite particle size during production, highlighting the beneficial relationship between reduced graphite particle size and improved mechanical properties.

Keywords: Piston materials; Graphite particle size; Mechanical properties; Metal composites; Scanning Electron Microscope

1. Introduction

One of the most common alloys used in car engines' cylinder heads, cylinder liners, pistons, and cylinders is hypereutectic Al-Si. It is due to a variety of advantageous characteristics, including high specific strength, low density, low coefficient of thermal expansion, corrosion resistance, and exceptional wear resistance [1]. The early aluminum-silicone alloy was notoriously brittle; dropping one by accident from bench height would typically cause a crack that was expensive, if not impossible, to fix. The weight-to-mass ratio of the alloy is increased when nickel is added, but the brittleness is decreased [2].

The eutectic Al-12%Si alloy that makes up the standard piston alloy has roughly 1% of Cu, Ni, and Mg in it [3]. Some eutectic alloys have been designed to be stronger at elevated temperatures. While they have less wear and thermal expansion, hypereutectic alloys with 18 and 24% Si are weaker [4]. Although primarily based on these fundamental alloy types, the provider of aluminum pistons really uses a broad range of more improved alloy compositions. As a result, gravity die casting is used to make the bulk of pistons [5]. Properly regulated solidification conditions and optimized alloy compositions enable the creation of lightweight and very structurally robust pistons. However, forged pistons made of eutectic and hypereutectic alloys are stronger and utilized in high-performance engines, which put the pistons under even greater strain [6]. With the same alloy composition, forged pistons have a finer microstructure than

* Corresponding author: Ayodele James Oyejide.

cast pistons, and their manufacturing technique yields higher strength at lower temperatures [7]. The ability to create thinner walls and, hence, lighter pistons is an additional benefit [2].

The use of graphite particles to improve the characteristics of piston materials has gained popularity in recent years. Graphite has the potential to be a promising reinforcement material for piston alloys because of its special combination of qualities, which include high thermal conductivity, lubricity, and chemical stability. Research is still being done to determine how graphite's particle size variation affects the mechanical characteristics of piston materials. The impact of graphite particles on the mechanical characteristics of piston materials has been the subject of numerous investigations [8–12]. For instance, research on the creation of piston composites based on aluminum and reinforced with graphite particles of various sizes demonstrates that the addition of graphite greatly enhanced the composites' tribological characteristics, lowering wear rates and friction coefficients [13]. In a similar vein, [14] investigated how particle size affected the wear resistance and heat conductivity of piston alloys. According to their findings, the lubricating effects of finer graphite particles resulted in increased wear resistance and higher heat conductivity.

Nevertheless, research is still being done to determine how graphite's particle size variation affects the mechanical characteristics of piston materials. This study examines the possible impact of different graphite particle sizes on the mechanical characteristics of pistons, which are essential parts of internal combustion engines. The process entails reducing graphite that is recovered from spent batteries by ball milling it for varying times, resulting in a composite that may be machined. We examined a machined ingot made from the melted piston to determine its mechanical properties using SEM analysis and particle size variation. Significant increases in mechanical properties are revealed by the subsequent tensile and hardness tests, especially in composites with reduced graphite particle sizes. A remarkable 53% increase in tensile strength and 2.5% enhancement in hardness was realized, underscoring the potential of optimizing piston performance by controlling graphite particle size during manufacturing.

2. Materials and Method

2.1. Sample collection and preparations

Locally, used batteries were gathered from different Ogbomoso junkyards and landfills. The batteries' carbon (graphite) rod was removed, cleaned, and ground into a fine powder. We obtained and gathered used pistons from neighboring auto shops. A number of preparations, including the extraction and milling of graphite at different times, the creation of an ingot from discarded pistons, the addition of graphite at different particle sizes to the composition of piston materials, particle size analysis, and mechanical testing, were carried out in order to examine the impact of particle size variation on the mechanical properties of piston materials.

2.2. Extraction and milling of graphite

As seen in Figure 1, the collected used batteries were arranged on a level surface. Using pliers, the carbon rods inside the batteries were removed. They were cleaned, rinsed, and dried with a drier made locally. As seen in Figure 2C, the dry carbon rods were ground with a grinding stone and then sieved to produce fine graphite particles. The fine graphite particles were ground for 9 hours. The graphite particles were ground using a ball milling machine and a dry milling technique with a ball-to-powder ratio (BPR) of 10:1 (seven large balls and three small balls, each with a diameter of 145 mm and 81 mm). During the milling process, certain amount of graphite particles was scooped every 3 hours. The time interval was used to vary the particle size of the graphite as the particles size reduces with increasing time of milling. The particle sizes were determine using the Endecott Test Sieve Shaker

Table 1 Materials and usage

S/N	Equipment	Function
1	Plier	Extracting carbon rods
2	Grinding stone	Grinding the carbon rod
3	Dryer	Absorbing the moisture in the carbon rod
4	Mesh	Obtaining a fine particle of the grinded carbon rod
5	Furnace	Melting
6	Weighing balance	Weighing

7	Grinding Machine	Polishing Specimen
8	Lathe machine	Machining Specimen
9	Hardness machine	Hardness test
10	Tensile testing machine	Tensile test
11	SEM machine	SEM
12	XRD machine	XRD
13	Optical emission spectrometer	Composition analysis
14	Tong	Picking hot billet

Figure 1 Utilized wastes (A) battery and (B) discarded pistons

2.3. Formation of Ingot from the discarded pistons

Figure 2 Process of producing the ingot. (A) melting of the discarded pistons (B) produced ingot (c) grinded carbon rods of the batteries (D) Machined specimen for experiment.

As illustrated in Figure 1B, the used pistons were continuously heated to 775 degrees Celsius by charging them into a pot inside the furnace while the furnace was kept open. The kettle fills with molten metal from leftover piston

components after another charge. Using tongs, the pot was removed from the furnace. As seen in Figure 2B, the molten metal was then poured into a mold to create the necessary ingot.

2.4. Microscopic and Analysis

The ingot underwent basic structural analysis using a scanning electron microscope (SEM), and its chemical composition was ascertained using an optical emission spectrometer (Model: MAXLMM06). In order to maintain an appropriate vacuum at the electron gun, SEM instruments place the specimen in a relatively high-pressure chamber with a short working distance and a distinct pump for the electron optical column. In the Environmental Scanning Electron Microscope (ESEM), the high-pressure area surrounding the sample neutralizes charge and amplifies the secondary electron signal. Since the Field Emission Guns (FEG) can produce small spots and high primary electron brightness even at low accelerating potentials, low voltage SEM is usually carried out in a FEG-SEM. For quantitative X-ray microanalysis or backscattered electron imaging of biological or material specimens, embedding in a resin and polishing it to a mirror-like finish can be employed [15]. Hence, using an energy dispersive spectroscopy system-equipped Carl Zeiss Smart Evo 10 scanning electron microscope, the microstructure and chemical compositions of the sample's phases were examined.

In addition, we used a Rigaku X-ray Diffractometer, Model: P1102, X-ray Diffractometer (XRD) to perform examinations of the graphite particles and the composite with the best mechanical properties. The sample was run through the Rigaku D/Max-IIIC X-ray diffractometer by setting the radiation for the Copper K-Alpha (CuK-α) was set at 40KV and 20mA, and the scanning rate was adjusted to produce diffractions at a rate of 2/min in the 2-to-50-degree range at room temperature.

2.5. Rule of Mixture

It was found that the majority element in the ingot's material makeup was aluminum. Therefore, using a technique known as the rule of mixes, the graphite particles of different sizes were combined in a ratio proportional to the percentage weight of aluminum in the ingot. Rule of mixture is a method of approach to approximate estimation of composite material properties, based on an assumption that a composite property is the volume weighted average of the phases (matrix and dispersed phase) properties [16]. Hence, the graphite particles were grouped into 3 different samples of:

Sample A = Graphite particles with 3hrs of milling

Sample B = Graphite particles with 6hrs of milling

Sample C= Graphite particles with 9hrrs of milling

$$\frac{1}{\rho_{AL+Gr}} = \frac{wt\%\ of\ aluminium\ alloy\ (\%Al)}{density\ of\ Al\ (\rho_{Al})} + \frac{wt\%\ of\ graphite}{\rho_{Gr}} \quad (1)$$

$$\rho_{Al} = density\ of\ Aluminium\ alloy = 2.7 g/cm^3$$

$$\rho_{Gr} = density\ of\ graphite = 2.2 g/cm^3$$

$$\text{wt\% of Al} + \text{wt\% of Gr} = 100\% \quad (2)$$

$$\rho_{Al+Gr} = density\ of\ the\ composite\ (Al + Gr) \quad (3)$$

Recall that:

$$\rho = \frac{m}{v} \quad (4)$$

$$m = \rho \times v \quad (5)$$

Where $v = \pi r^2 h$

v = volume of mould

$$r = \frac{d}{2} \quad (6)$$

Where d = diameter of mould

h = length of mould

$$m_{Al+Gr} = \rho_{Al+Gr} \times v \quad (7)$$

$$m_{Al} = wt\%\ of\ Al \times m_{Al+Gr}$$

$$m_{Gr} = wt\%\ of\ Gr \times m_{Al+Gr}$$

Considering 2wt% of graphite

$$\frac{1}{\rho_{Al+Gr}} = \frac{0.98}{2.7} + \frac{0.02}{2.2}$$

$$\frac{1}{\rho_{Al+Gr}} = 0.3721$$

$$\rho_{Al+Gr} = \frac{1}{0.3721}$$

$$\rho_{Al+Gr} = 2.69 g/cm^3$$

$$r = \frac{12}{2} = 6mm = 0.6cm$$

$$r = 150mm = 15cm$$

$$v = \pi \times 0.6^2 \times 15$$

$$v = 16.93cm^3$$

$$m_{Al+Gr} = 2.69 \times 16.96$$

$$= 45.68g$$

$$m_{Al} = 0.98 \times 45.68g$$

$$= 44.77g$$

$$m_{Gr} = 0.02 \times 45.68$$

$$= 0.91g$$

Furthermore, a mass of 45.68g of aluminum alloy was charged into the pot and heated to approximately 775°C in the furnace. Sample A, weighing 0.89g, was added to the aluminum alloy's molten metal and properly mixed. After the combination was melted, it was put into a mold to create a rod, which was then machined into specimen A, which was needed for mechanical testing. To create specimens B, C, and D, respectively, the procedure was repeated using the remaining samples (B and C) of graphite particles. A further 45.68g of aluminum alloy was weighed and charged into the pot, which was then heated to roughly 775°C in the furnace. The molten metal of aluminium without dispersion of graphite particles was then poured in a mould to form a rod that was machined to required control specimen for mechanical testing (Figure 2D).

2.6. Tensile test

The machined specimens were subjected to a tensile test at room temperature using an Instron Extensometer (model: E1-F1-G1, system ID: 3369S3407). The ultimate tensile strength (UTS), which is stated below, was obtained using the data table from the tension test/graph.

$$UTS = \frac{P_{max}}{A_o} \quad 8$$

Where $P_{max} = maximum\ load\ applied\ (N)$

$$A_o = Original\ cross - sectional\ area\ (m^2)$$

$$A_0 = \frac{\pi d_o^2}{4} \quad 9$$

$$d_o = gauge\ diameter\ (mm)$$

The percentage elongation after fracture was obtained from equation

$$\varepsilon = \frac{l_u - l_o}{l_o} \times 100 \quad 3.10$$

$$l_o = original\ length\ (mm)$$

$$l_u = final\ gauge\ length\ (mm)$$

3. Results and discussions

The elemental makeup of piston materials (ingot) and the proportion of each element in the ingot are displayed in Table 2. Al makes up the majority of the composition (85%), with additional elements including Si, Copper (Cu), Magnesium (Mg), Iron (Fe), Calcium (Ca), Chromium (Cr), and Zinc (Zn) also present. The documented gross faults in the castings were observed using SEM, and Figure 3 displays the SEM of the ingot. Table 3 displays the results of the Endecott Test Sieve Shaker used to determine the different graphite particle sizes, and Figure 3A illustrates the effects of the samples A, B, and C's particles after sieving.

A Rigaku D/Max-111C X-ray diffractometer was used to determine the phase of the graphite particle and the composite with the best mechanical properties. Diffractions were performed at a scanning rate of 20 /min in the 2 to 500 range at room temperature, using a CuKa radiation source at 40Kv and 20Ma. Figures 3B and C, respectively, show the XRD graphite particles and sample C (Al alloy + graphite particle milled for 9 hours).

Table 2 Result of chemical composition of the piston materials (ingot)

Element	Composition (%)
Al	85.0
Si	11.37
Cu	1.21
Mg	0.828
Ni	0.658
Fe	0.544
Mn	0.106
Zn	0.0976
Ti	0.0489
Cr	0.0314

Pb	0.0117
Ga	0.0117
V	0.0096
Sn	0.0093
P	0.0071
Zr	0.0042
Sb	0.0041
Pr	0.0019
Ca	0.00033
Others	0.04617

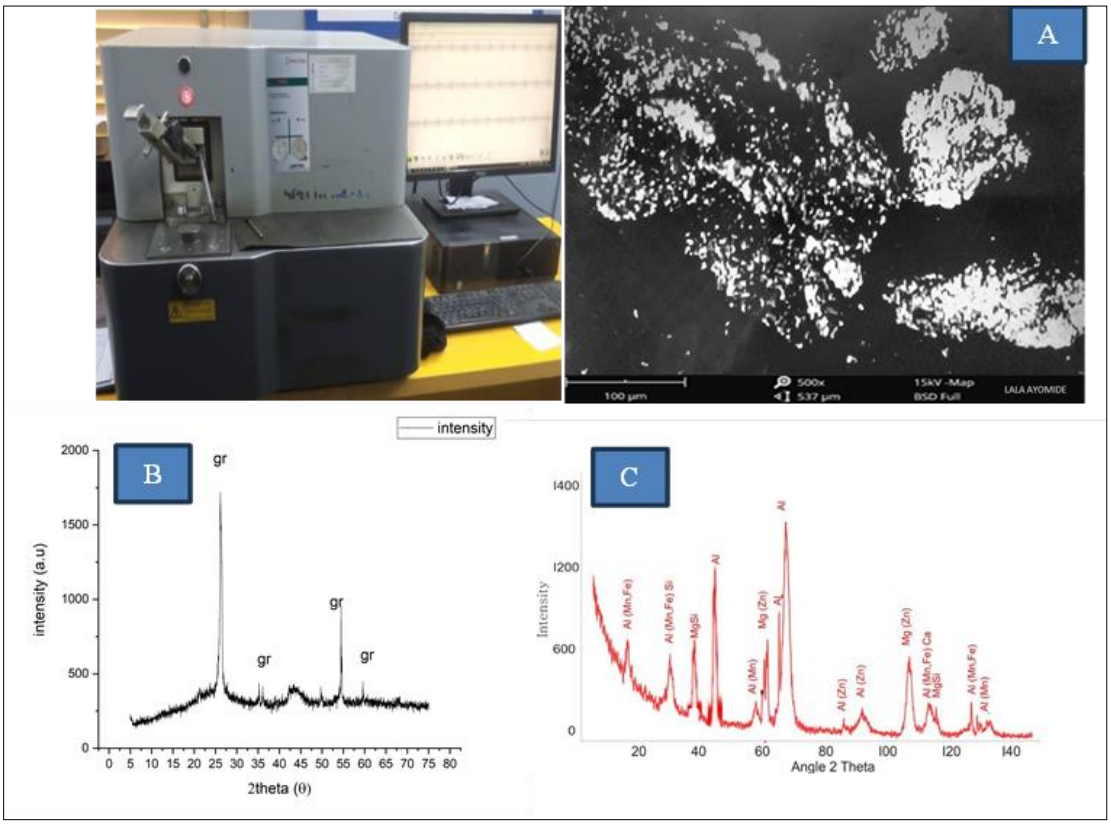

Figure 3 (A) SEM result of particle variation (B) EDX for XRD graphite particles (C) Al alloy + graphite particle.

Table 3 Result of various particle sizes of graphite

Graphite sample	Milling time (Hrs)	Particle size (μm)
A	3	125
B	6	>90
C	9	<90

The specimens' tensile strength is shown in Table 4. The specimens A, B, and C, as well as the control specimen, had tensile strengths of 91.63 MPa, 23.10 MPa, 72.27 MPa, and 140.44 MPa, respectively. The tensile strength of the control sample was found to increase from 91.63 MPa to 140.44 MPa with the addition of graphite particle milled for nine hours.

In contrast, the tensile strength decreased from 91.63 MPa to 23.10 MPa and from 91.63 MPa to 72.27 MPa with the addition of milled graphite for three and six hours, respectively.

Furthermore, the yield strength values were computed using the tensile data obtained from the experimental outcome. Table 5 illustrates how the yield strength of the specimens varies, with specimen C having the highest yield strength of 60 Mpa and specimen A having the lowest yield strength of 15 Mpa. Table 6 displays the elastic modulus, which is determined by taking the tensile strength and tensile strain values. The modulus of elasticity is found to be lowest at specimen A (value 14259.25 Mpa) and highest at the control specimen (value 35242.31 Mpa). Additionally, Table 7 displays the percentage elongation that is determined using the values of tensile strength and tensile strain. The specimen C exhibits the maximum percentage elongation, measuring 0.55%, whereas specimen A displays the lowest percentage elongation, measuring 0.16%.

Table 4 Results of tensile strength carried out on the specimens

Specimen	Tensile strength (Mpa)
Control	91.63
A	23.10
B	72.27
C	140.44

Table 5 Results of the yield stress of the specimen

Specimen	Yield Stress (MPa)
Control	40
A	15
B	25
C	60

Table 6 Results of the elastic modulus of the specimens

Specimen	Elastic modulus (MPa)
Control	35242.31
A	14259.25
B	34913.04
C	25721.61

Table 7 Result of percentage elongation of the specimens

Specimen	Percentage elongation (%)
Control	0.25
A	0.16
B	0.20
C	0.55

The results of the tensile tests carried out on the specimens using the Instron Extensometer are shown in Figure 4.

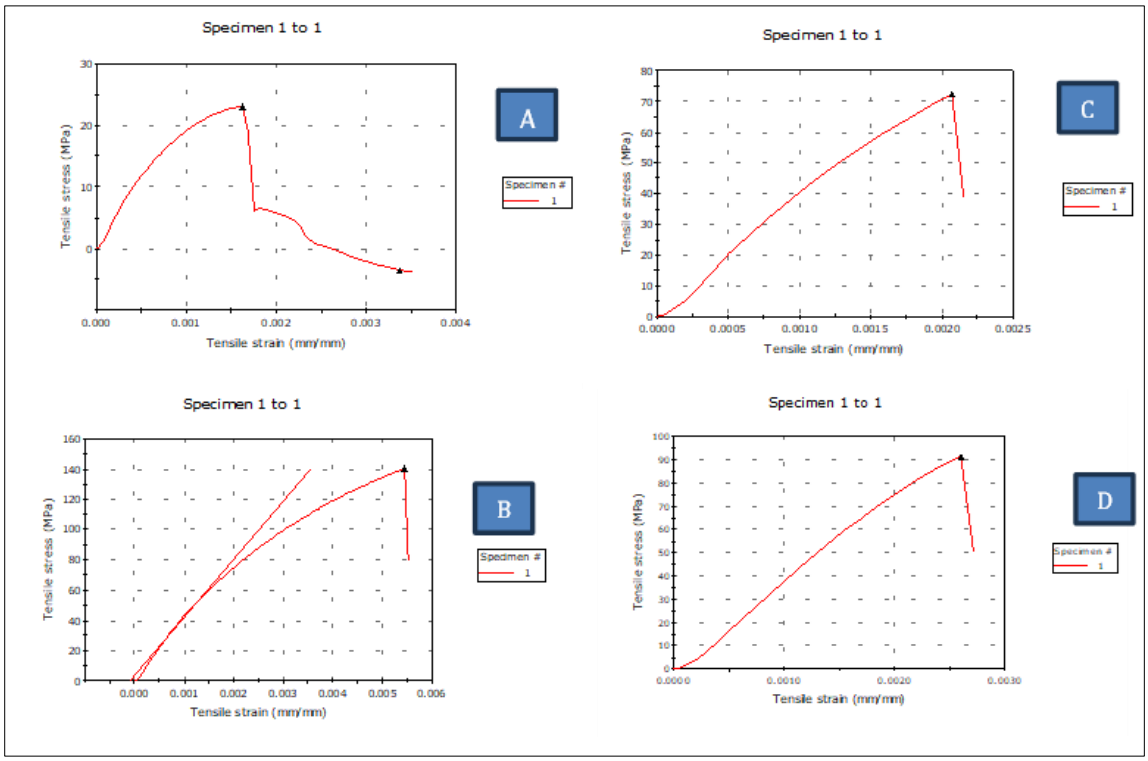

Figure 4 Tensile stress versus tensile strain for (A) control (B) specimen A (C) specimen B and (D) specimen C, respectively.

Table 8 displays the variation of the hardness qualities based on the trial runs. The mean of the measurements made on each sample at three different points was used to calculate the hardness values. The control specimen, specimens A, B, and C have corresponding hardness values of 57.97HRB, 47, 59.4HRB, and 48.67HRB. The control sample's hardness increased from 57.97HRB to 59.4HRB with the addition of graphite particle milled for 6 hours, but the hardness decreased from 57.97HRB to 47HRB and 57.97HRB to 48.67HRB with the addition of graphite milled for 3 hours and 9 hours, respectively.

Furthermore, we observed the mechanical property comparison according to the number of milling hours. Table 9 displays the changes in graphite's tensile strength, hardness, and particle size throughout milling hours. Tensile strength was seen to rise as milling hours increased, as Figure 5 illustrates, since the graphite particle size decreased as milling hours increased. The composite material that contains Al and graphite and is milled for nine hours has the maximum tensile strength. Additionally, Figure 5 showed that the composite with the maximum hardness was made of Al combined with graphite and milled for six hours.

Table 8 Results of hardness test carried out on the specimens

Specimen	Point 1	Point 2	Point 3	Mean
Control	62.5	60.4	51	57.97
A	48	49	46	47
B	58	58	62.3	59.4
C	49.5	51	45.5	48.67

Table 9 Tensile strength, hardness and particle size as a function of milling time

Specimen	Particle size (µm)	Milling time (Hrs)	Tensile strength (MPa)	Hardness (Brinell)
A	125	3	23.10	47
B	90	6	72.27	59.43
C	<90	9	140.44	48.67

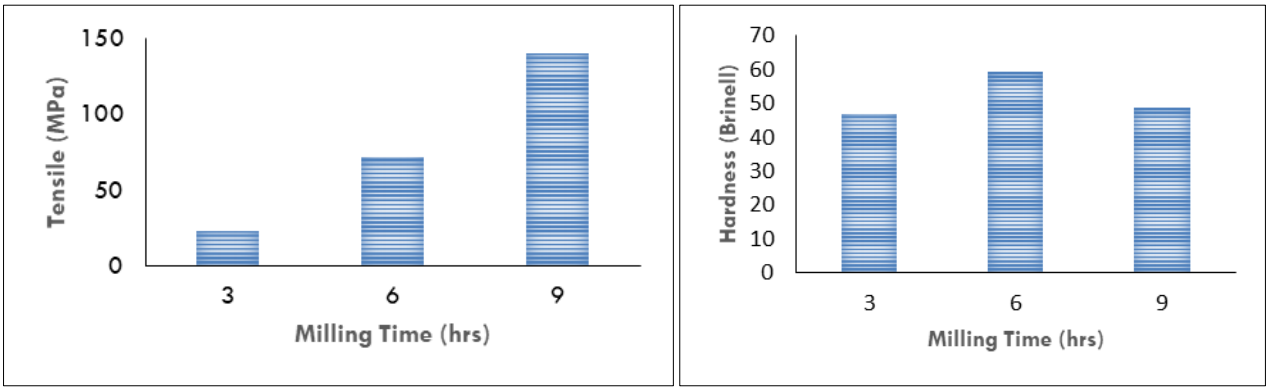

Figure 5 Variation in tensile strength with respect to varying milling hours and particle size of the graphite**.**

4. Conclusion

Stir casting was used to successfully introduce graphite at different particle sizes to the piston material (Al alloy) matrix. We examined how the mechanical characteristics and microstructure behaved in connection to the quantity of graphite particles present. Comparing the composite (Al alloy with graphite ground for nine hours) to the piston material without graphite, the composite's tensile strength rose by 53%. When compared to piston material without graphite, the composite (Al alloy with graphite milled for six hours) has a 2.5% higher hardness value. Nevertheless, when compared to pure aluminum alloy, aluminum alloys milled with graphite for three and nine hours exhibit a significant drop in hardness values. Tensile values of aluminum that has been machined for three and six hours also decrease. The results of the study showed that future research should aim to lower the particle size of graphite if improved mechanical properties of the piston are sought. Additionally, the study shows how the waste composites can be effectively exploited to produce metals for use in regional fabrications.

Compliance with ethical standards

Disclosure of conflict of interest

The authors declare that there is no conflict of interest.

References

[1] A. Audu, A. Mamoon and N.N. Yunusa. “Production of Motorcycle Piston with Improved Mechanical Properties and Wear Resistance using Scrap Aluminium Alloys.” American Journal of Engineering Research (AJER, 8(3), 57–63, 2019.

[2] European Aluminium Association. (2011). Aluminium Pistons. In European Aluminium Association.

[3] S. Xu, K. Khanlari, B. Lin, T. Fan, S. Xia, I.E. Achouri, W. Zhang, and Y. Jiang, "Effects of Fe-Addition as a Beneficial Modifying Element on the Microstructure and Mechanical Properties of an Al–Si–Cu–Mg–Ni–Mn Piston Alloy," Metallography, Microstructure, and Analysis, vol. 12, no. 3, pp. 401-412, 2023.

[4] K. Tiwari, G. Gautam, N. Kumar, A. Mohan, and S. Mohan, "Effect of primary silicon refinement on mechanical and wear properties of a hypereutectic Al-Si alloy," Silicon, vol. 10, pp. 2227-2239, 2018.

[5] B.K. Kosgey, S.M. Maranga, J.M. Kihiu, and Y. Ando, "Investigation on Hardness of Gravity Die Cast Secondary Al-10Si Piston Alloy with Trace Addition of Sr, Fe and Mn," 2016.

[6] U. Singh, J. Lingwal, A. Rathore, S. Sharma, and V. Kaushik, "Comparative analysis of different materials for piston and justification by simulation," Materials Today: Proceedings, vol. 25, pp. 925-930, 2020.

[7] L. Kerni, A. Raina, and M.I.U. Haq, "Performance evaluation of aluminium alloys for piston and cylinder applications," Materials Today: Proceedings, vol. 5, no. 9, pp. 18170-18175, 2018.

[8] J. Narciso, J.M. Molina, A. Rodríguez, F. Rodríguez-Reinoso, and E. Louis, "Effects of infiltration pressure on mechanical properties of Al–12Si/graphite composites for piston engines," Composites Part B: Engineering, vol. 91, pp. 441-447, 2016.

[9] P. Sharma, S. Sharma, R. Kumar Garg, K. Paliwal, D. Khanduja, and V. Dabra, "Effect of graphite content on mechanical properties and friction coefficient of reinforced aluminum composites," Powder Metallurgy and Metal Ceramics, vol. 56, pp. 264-272, 2017.

[10] H. Faleh, N. Muna, and F. Ştefănescu, "Properties and applications of aluminium-graphite composites," Advanced Materials Research, vol. 1128, pp. 134-143, 2015.

[11] R. Dalmis, H.A.M.D.U.L.L.A.H. Cuvalci, A.Y.K.U.T. Canakci, and O.N.U.R. Guler, "Investigation of graphite nanoparticle addition on the physical and mechanical properties of ZA27 composites," Advanced Composites Letters, vol. 25, no. 2, p. 096369351602500202, 2016.

[12] K.P.Y. Sreekanth, G.K.P. Yadav, and Y.G.K. Prasad, "Experimental Evaluation of Piston using Aluminium Alloy (LM24) Reinforced with SiC and Graphite," International Journal of Mechanical and Production Engineering Research and Development, vol. 9, pp. 445-456, 2019.

[13] P.K. Yadav, S.K. Patel, V.P. Singh, M.K. Verma, R.K. Singh, B. Kuriachen, and G. Dixit, "Effect of different reinforced metal-matrix composites on mechanical and fracture behaviour of aluminium piston alloy," Journal of Bio-and Tribo-Corrosion, vol. 7, no. 2, p. 54, 2021.

[14] I. Alshalal, H.M.I. Al-Zuhairi, A.A. Abtan, M. Rasheed, and M.K. Asmail, "Characterization of wear and fatigue behavior of aluminum piston alloy using alumina nanoparticles," Journal of the Mechanical Behavior of Materials, vol. 32, no. 1, p. 20220280, 2023.

[15] A. Mohammed and A. Abdullah, "Scanning electron microscopy (SEM): A review," in Proceedings of the 2018 International Conference on Hydraulics and Pneumatics—HERVEX, Băile Govora, Romania, November 2018, pp. 7-9.

[16] A. Ul-Hamid and A. Ul-Hamid, "Sample preparation," in A Beginners' Guide to Scanning Electron Microscopy, pp. 309-359, 2018.

[17] B. Samir, M. Belkacem, and G. Brahim, "Numerical Modeling of the Effects of Fiber Packing and Reinforcement Volume Ratio on the Transverse Elasticity Modulus of a Unidirectional Composite Material Glass/Epoxy," Journal of Composite & Advanced Materials/Revue des Composites et des Matériaux Avancés, vol. 30, 2020.